Published in final edited form as:
Cell Stem Cell. 2015 January 8; 16(1): 51–66. doi:10.1016/j.stem.2014.11.004.

Perivascular Gli1+ progenitors are key contributors to injury-induced organ fibrosis

Rafael Kramann[1,2,*], **Rebekka K. Schneider**[3], **Derek P. DiRocco**[1], **Flavia Machado**[1], **Susanne Fleig**[1], **Philip A. Bondzie**[4], **Joel M. Henderson**[4], **Benjamin L. Ebert**[3,5], and **Benjamin D. Humphreys**[1,5,*]

[1]Renal Division, Brigham and Women's Hospital, Department of Medicine, Harvard Medical School, Boston, Massachusetts, 02115, USA

[2]Division of Nephrology and Clinical Immunology RWTH Aachen University Medical Faculty RWTH Aachen University, Pauwelsstrasse 30, 52074 Aachen, Germany

[3]Division of Hematology, Brigham and Women's Hospital, Department of Medicine, Harvard Medical School, Boston, Massachusetts, 02115, USA

[4]Department of Pathology and Laboratory Medicine, Boston University School of Medicine, Boston, Massachusetts, 02118, USA

[5]Harvard Stem Cell Institute, Cambridge, Massachusetts, 02138, USA

Summary

Mesenchymal stem cells (MSCs) reside in the perivascular niche of many organs, including kidney, lung, liver, and heart, although their roles in these tissues are poorly understood. Here, we demonstrate that Gli1 marks perivascular MSC-like cells that substantially contribute to organ fibrosis. In vitro, Gli1+ cells express typical MSC markers, exhibit trilineage differentiation capacity, and possess colony-forming capacity, despite constituting a small fraction of the platelet-derived growth factor-β (PDGFRβ)+ cell population. Genetic lineage tracing analysis demonstrate that tissue-resident, but not circulating, $Gli1^{+}$ cells proliferate following kidney, lung, liver, or heart injury to generate myofibroblasts. Genetic ablation of these cells substantially ameliorates

*Correspondence to: Benjamin D Humphreys, MD, PhD, Renal Division, Brigham and Women's Hospital, Department of Medicine, Harvard Medical School, Boston, Massachusetts; 77 Avenue Louis Pasteur, 02115, Boston, MA, Phone: 617-525-5971, Fax: 617-525-5965, bhumphreys@partners.org Or Rafael Kramann, MD, Renal Division, Brigham and Women's Hospital, Department of Medicine, Harvard Medical School, Boston, Massachusetts; 77 Avenue Louis Pasteur, 02115, Boston, MA, Phone: 857-210-5633, Fax: 617-525-5965, rkramann@gmx.net.

Supplemental Information
Supplemental Information includes Supplemental Experimental Procedures, seven figures and one table can be found with this article online.

Author contributions
R.K. designed and carried out experiments, analyzed results and wrote the manuscript, R.K.S., D.P.D. F.M., SF, P.B. and J.M.H. carried out experiments, analyzed the data and reviewed the manuscript, B.L.E. designed experiments and reviewed the manuscript, B.D.H. designed experiments, interpreted results and wrote the manuscript

kidney and heart fibrosis, and preserves ejection fraction in a model of induced heart failure. These findings implicate perivascular Gli1$^+$ MSC-like cells as a major cellular origin of organ fibrosis and demonstrate these cells may be a relevant therapeutic target to prevent solid organ dysfunction following injury.

Introduction

More than half a century ago it was noted that subcutaneously implanted bone marrow cells formed bone (Danis, 1957). Once isolated, the cell type responsible for this effect was termed mesenchymal stem cells (MSC) in reference to multipotent cells within bone marrow capable of giving rise to mesenchymal tissues (Caplan, 1991). These MSC possess stem cell characteristics including self-renewal and clonogenic capacity (Caplan and Correa, 2011). In recent years MSC have been isolated from virtually all postnatal and fetal tissues including placenta, adipose tissue, muscle, umbilical cord, skin, dental pulp, tendon and characterized *in vitro* (Murray et al., 2014). Vasculature represents the *in vivo* niche of MSC, helping to explain why MSC have such a broad tissue distribution (Crisan et al., 2008). However, our current knowledge about MSC is almost entirely based on *in vitro* observations of cultured MSC. The term MSC-like is used to refer to cells *in vivo* that are perivascular and give rise to typical cultured MSC, that possess trilineage differentiation potential, a defined surface marker expression pattern and a spindle-shaped appearance. MSC-like cells localize to the pericyte niche in microvasculature, where they make close contact to endothelial cells, and they also reside in the adventitia of larger vessels, where they do not contact endothelia (Murray et al., 2014).

Exogenously infused MSC modulate tissue injury and repair, largely through paracrine secretion of anti-apoptotic, anti-scarring, pro-angiogenic and immunomodulatory factors involved in tissue regeneration (Caplan and Correa, 2011). These properties have led to novel therapeutic strategies involving exogenous administration of MSC in various injury and disease settings. Almost 400 clinical trials involving exogenous MSC are ongoing or have been performed (www.FDA.gov). Despite the broad therapeutic potential of this cell type, the in vivo role of perivascular MSC-like cells remains undefined due to the absence of specific *in vivo* markers. Recently Zhao et al. demonstrated that Gli1 is just such a marker of perivascular MSC-like cells in the mouse incisor (Zhao et al., 2014). Gli1$^+$ incisor cells express typical MSC surface markers in culture and possess trilineage differentiation capability. Using a Gli1-CreER^{t2} genetic fate tracing approach, the authors showed that following incisor injury newly formed dentin tubules derive from Gli1$^+$ cells.

We demonstrate that, in mice, perivascular Gli1$^+$ cells from bone-marrow, muscle, heart, lung, liver and kidney express a typical MSC marker pattern *in vivo*, are plastic adherent and possess trilineage differentiation capability towards chondrocytes, osteoblasts and adipocytes *in vitro*. Gli1$^+$ cells form an extensive perivascular network and possess increased colony forming unit capability. Following organ injury these resident Gli1$^+$ cells are committed to the myofibroblast lineage. Genetic ablation of Gli1$^+$ cells ameliorates fibrosis and improves organ function, providing a proof-of-principle for therapeutic targeting of this cell type in fibrotic disease.

Results

Gli1$^+$ cells form an extensive network around the vasculature, express a typical MSC marker pattern in vivo and possess trilineage differentiation capability *in vitro*

While examining expression of Hedgehog (Hh) pathway constituents, we observed that Gli1 is specifically expressed in cells surrounding vasculature, from microvascular capillaries to large arteries (Figure S1A). The perivascular localization and low frequency of these cells suggested a possible MSC-like identity, similar to the recent report that Gli1 marks mouse incisor MSCs (Zhao et al., 2014).

To comprehensively assess the distribution of these cells in solid organs and tissues, we crossed Gli1-CreER^{t2} driver mice to a tdTomato-reporter for inducible genetic labeling. Gli1-CreER^{t2}; R26tdTomato mice were pulsed with tamoxifen at 8 weeks and 48 hours later Gli1$^+$ cells were identified in the perivascular niche across all tissues tested (Figure 1A–C). Immunostaining for endogenous Gli1 protein and Gli1 mRNA expression of sorted cell populations validated this model (Figure S1B–C). Gli1$^+$ cells formed an extensive perivascular network (1) localized in the adventitia of large arteries (Figure 1A) and arterioles (Figure 1C arrows) distant from endothelial cells (adventitial niche) and (2) intimately associated with the microvasculature in direct contact to CD31$^+$ endothelial cells (Figure 1C, arrowheads). Immunogold staining and electron microscopy confirmed that Gli1$^+$ cells lie directly adjacent to endothelial cells (Figure 1B). Gli1$^+$ cells were also positioned around biliary ducts of the liver and around larger airways of the lung (Figure 1C, asterisk). Gli1$^+$ cells consistently expressed the mesenchymal marker PDGFR-β (Figure 1A,C). In contrast to mouse incisor where Gli1$^+$ cells are predominantly peri-arterial (Zhao et al., 2014), we found that many Gli1$^+$ cells also exist in a pericyte niche adjacent to endothelial cells of muscle, bone-marrow, lung, heart, kidney and liver. To better define the relationship of Gli1$^+$ cells relative to vasculature, we performed fluorescence microangiography (FMA), (Kramann et al., 2014). This demonstrated very close apposition of Gli1$^+$ cells around capillaries in both heart and kidney, with tdTomato$^+$ cell processes wrapping around fluorescent microbead filled capillaries (Movies S1– S2).

We employed fluorescence-activated cell-sorting (FACS) of whole digested organs and tissues to define the overall frequency of Gli1$^+$ cells (Figure 1D). To characterize Gli1$^+$ cells by accepted criteria defined for MSC, we cultured sorted Gli1$^+$ cells and determined that they had trilineage differentiation capacity towards chondrocytes, adipocytes and osteoblasts regardless of their origin (Figure 1D). Further, we performed whole organ flow cytometry without pre-culture of the cells and confirmed the expression of a typical mouse MSC marker pattern (Boxall and Jones, 2012; Pelekanos et al., 2012) on Gli1$^+$ cells *in vivo* (Figure 1E). Importantly, Gli1$^+$ cells were negative for the endothelial cell marker CD31 and the hematopoietic lineage marker CD45 while we observed low levels of CD34 expression in some organs (Figure 1E). Furthermore, we assessed the expression of other markers that have been described for MSC and/or pericytes by immunostaining of tissues. We demonstrated that Gli1$^+$ cells do not express significant levels of NG2, CD73, CD146 and STRO1, while we observed expression of 3G5, Nestin and PDGFRα (Figure S1D). These

experiments show that Gli1$^+$ cells express typical markers and are a source of MSC-like cells across all organs tested.

Gli1$^+$ cells line the endosteum and vascular sinusoids in the bone marrow and retain a typical MSC surface pattern in culture

In the bone marrow niche, MSC surround blood vessels and sinusoids but also line endosteum (Morrison and Scadden, 2014). We observed Gli1$^+$ cells lining CD31$^+$ endothelial cells of bone marrow sinusoids as well as endosteum of the compact bone (Figure 2A), representing both the vascular and the endosteal niche. Since mouse bone marrow MSC in the endosteal niche cannot readily be isolated from the bone marrow, we applied an endosteal bone chip culture method. Interestingly, Gli1$^+$ cells migrated out of the bone fragments and proliferated in the culture dish (Figure 2B). Flow cytometric analysis of these cells indicated that ~32% had a Gli1$^+$ origin (Figure 2C). MSC isolated from bone chips (BM-MSC) as well as isolated from the myocardium (heart, H-MSC) maintained a typical MSC surface pattern with expression of CD44, CD29, CD105, Sca1 and absence of CD31, CD45, CD34 in culture (Figure 2C–D). Furthermore, Gli1$^+$ cells from bone, heart and kidney retained expression of 3G5, Nestin, PDGFRα and gained expression of CD146 and CD73, while we did not detect significant expression of NG2 or STRO1 in culture (Figure S2). These data suggest that Gli1$^+$ cells in culture are similar despite their origin from different organs.

Gli1$^+$ cells represent only a small fraction of the PDGFR-β$^+$ cell population with increased colony forming unit capability

Our results had indicated that Gli1 expression in adult mice defines PDGFRβ$^+$ MSC-like perivascular cells. However, a critical question was whether there were any functional differences between Gli1$^+$ cells and Gli1$^-$, PDGFRβ$^+$ cells. Flow cytometric analyses of whole organs indicated that all Gli1$^+$ cells express PDGFRβ but they represent only a small fraction of the total PDGFR-β$^+$ population (Figure 3A).

We next asked whether Gli1$^+$ cells differ in their clonogenic potential from Gli1$^-$ PDGFRβ$^+$ and PDGFRβ$^-$Gli1$^-$ cells. We sorted these populations from lung, heart, kidney and cultured bone chips and assessed colony formation after 2 weeks. Indeed, the clonogenic frequency of the Gli1$^+$PDGFRβ$^+$ fraction was significantly higher than that of the other populations across tissues tested (Figure 3B–C). Furthermore, colonies from the Gli1$^+$, PDGFRβ$^+$ fraction were substantially larger (Figures 3D, S3A). Gli1$^+$ cells showed stable growth over many passages *in vitro* (cells were grown for >30 passages from bone chips, >10 passages from all other organs).

Gli1$^+$ cells constitutively express Gli *in vitro* while pharmacologic inhibition of Gli reduces their colony forming unit capability

Gli1$^+$ cells retain significant mRNA expression of most Hh pathway members *in vitro* including Gli1–3 (Figure S3B). Given reported roles for Hh signaling in cell proliferation, we next investigated whether inhibition or activation of Hh signaling affects the CFU-F capability of Gli1$^+$ cells. Exogenous Shh increased Gli1 protein and colony number, and the smoothened inhibitor cyclopamine blocked this effect but cyclopamine alone had no effect

arguing against autocrine Hh ligand secretion (Figure 3E–F). By contrast, targeting Gli directly with the small molecule antagonist GANT61 decreased Gli1 protein levels and also decreased CFU-F capacity (Figure 3E–F). These results suggest constitutive expression of Gli1 in MSC-like cells *in vitro*. That direct inhibition of Gli reduced clonogenic capacity also implicates Gli in the self-renewal of $Gli1^+$ progenitor cells.

Perivascular $Gli1^+$ cells expand and become myofibroblasts after injury of major organs

The MSC is most commonly defined as a cell with trilineage differentiation capability and CFU-F capacity *in vitro* (Park et al., 2012). Our results thus far suggested that $Gli1^+$ cells in adult mice fulfill these criteria among organs tested and additionally express an MSC surface pattern *in vivo*. It has been proposed that MSC in the perivascular niche become activated upon organ injury and support tissue regeneration after injury (Caplan and Correa, 2011). This prompted us to perform fate-tracing and ablation studies of $Gli1^+$ cells following injury to major organs including kidney (unilateral ureteral obstruction, UUO and severe bilateral ischemia reperfusion injury, IRI), heart (angiotensin-2, AT2-induced myocardial fibrosis, ascending aortic constriction, AAC), liver (carbon tetrachloride, CCL4 induced fibrosis) and lung (intratracheal bleomycin instillation). To track the fate of genetically labeled $Gli1^+$ cells, we labeled them via tamoxifen administration and followed their fate in various organ injury models for up to 52 days. The injury was induced at least 10 days after tamoxifen administration to eliminate any possibility of recombination after injury (Goritz et al., 2011).

In both models of kidney injury we observed a dramatic increase of $Gli1^+$ cells in the medulla, the inner cortex and around arteries throughout the kidney and to a lower extent in the outer cortex (Figures 4A and S4A–C). The proliferative expansion and distribution of $Gli1^+$ cells following kidney injury suggested that they may differentiate into myofibroblasts. One of the defining features of myofibroblasts is expression of alpha-smooth muscle actin (α-SMA), and indeed most $Gli1^+$ cells acquired expression of α-SMA after injury (Figure 4A, S4A–C). Thus $Gli1^+$ cells proliferate and differentiate into myofibroblasts in kidney fibrosis.

To exclude the possibility that ‘leaky’ recombination might label cells that activate Gli1 expression following injury, we performed UUO surgery in bigenic Gli1CreER^{t2}; tdTomato mice without tamoxifen injection. There was no significant recombination under these conditions (Figure S4D–F). We also excluded the possibility that residual tamoxifen might label $Gli1^+$ cells following injury by extending the time between tamoxifen administration and UUO surgery from 10 days to 3 months. Importantly, the frequency of labeled cells following UUO was comparable to our original experiments, indicating that recombination was not occurring after surgery (Figure S4D–F). We also counterstained fibrotic kidneys following UUO and demonstrated that indeed all myofibroblasts (~96% of α-SMA$^+$ cells) express PDGFRβ (Figure S4H–I), consistent with a recent report (Henderson et al., 2013),

Cardiac fibrosis in the AT2-induced hypertensive heart disease model primarily affects coronary arteries and arterioles with extensions of collagen from the perivascular space into the cardiac interstitium (Weber et al., 1995) and this is what was observed in Gli1CreER^{t2}; tdTomato mice (Figure 4B). Fate tracing experiments revealed expansion of $Gli1^+$ cells in

the perivascular space where the vast majority of Gli1$^+$ cells differentiated into α-SMA positive myofibroblasts (Figure 4B–D). We also used AAC surgery to induce pressure-overload heart failure as a second model with perivascular but also interstitial myocardial fibrosis. In this case we observed both perivascular Gli1$^+$ expansion but also expansion of Gli1$^+$ cells in the cardiac interstitium distant from arteries and arterioles (Figure 4E–I) that also differentiated into α-SMA positive myofibroblasts (Figure 4G,I).

Large interstitial Collagen I-positive fibrotic areas were entirely full of Gli1$^+$ cells (Figure S4J), consistent with matrix secretion by Gli1$^+$ cells, prompting us to ask whether Gli1$^+$ cells mediate scarring following myocardial infarction. Indeed after coronary artery ligation the entire left ventricular scar area was full of α-SMA positive Gli1$^+$ cells (Figure S4K–M). We next quantitated the contribution of Gli1$^+$ cells to the myofibroblast pool in kidney and heart. This analysis revealed that ~45% of myofibroblasts in the kidney and ~60% of cardiac myofibroblasts derived from Gli1$^+$ progenitors (Figure S5A). Given the significant contribution of Gli1$^+$ cells to the myofibroblast pool in heart and kidney we then asked whether Gli1$^+$ cells also contribute to the myofibroblast pool following liver and lung injury. Indeed, we observed significant expansion and differentiation into α-SMA$^+$ cells following liver and lung injury (Figure 5A–F). Gli1$^+$ cells contributed to ~37% of α- SMA$^+$ interstitial cells following lung injury and ~39% of interstitial α-SMA$^+$ cells in liver fibrosis (Figure S6G).

Following injury of major organs Gli1$^+$ cells expanded through proliferation (S6A–F) and the majority of Gli1$^+$ cells acquired α-SMA expression (Figures 4–5), suggesting that perivascular Gli1$^+$ cells are committed to the myofibroblast lineage after injury. In line with these *in vivo* fate tracing studies, isolated FACS purified Gli1$^+$ cells from healthy bone marrow or heart did not express α-SMA 7 days after isolation. However, treatment with transforming growth factor beta (TGF-β) resulted in significant up-regulation of α-SMA mRNA and expression of α-SMA$^+$ stress fibers (Figure 5G–J).

Gli1$^+$ cells do not express NG2 in homeostasis or fibrosis but acquire NG2 expression during angiogenesis

Although not all pericytes express NG2 (Song et al., 2005; Stark et al., 2013), NG2 has been proposed as a marker of mature pericytes by some authors (Song et al., 2005). With an important role in angiogenesis where it promotes endothelial cell migration and proliferation (Fukushi et al., 2004; Stallcup, 2002), NG2 expression may not be static but rather induced in pericytes during angiogenesis and microvascular remodelling (Murfee et al., 2006). By contrast, many pericytes might show reduced or no expression of NG2 during homeostasis. In tumors, it has been demonstrated that PDGFRβ$^+$/NG2$^-$ perivascular cells can differentiate into mature NG2$^+$ pericytes (Song et al., 2005). Moreover, recent work suggests that during injury and repair of the mouse incisor, Gli1$^+$ progenitors differentiate into NG2$^+$ mature pericytes. Interestingly, the authors also demonstrated that Gli1$^+$ cells give rise to the entire MSC population from the mouse incisor, whereas NG2$^+$ cells only contribute a minor subpopulation (Zhao et al., 2014). These data suggested that Gli1 expression may define immature perivascular cells, distinct from mature NG2$^+$ pericytes, and constitute the major progenitor pool for MSC. We therefore asked whether Gli1$^+$ cells could acquire expression

of NG2 during fibrosis. Interestingly, we observed that only a small fraction of Gli1$^+$ cells expressed NG2 (~5%) and this fraction actually decreased following UUO or AAC (Figure S5B). Of note, Gli1$^+$ cells retained expression of other pericyte/MSC markers 3G5, PDGFRα, PDGFRβ and Nestin during fibrosis *in vivo* (Figure S5C).

Given a reported role for NG2 in angiogenesis (Fukushi et al., 2004), we next asked whether Gli1$^+$ cells gain NG2 expression following myocardial infarction since angiogenesis is involved in the repair process of this model. Indeed, we observed Gli1$^+$ cells expressing NG2 and CD146 assembling vascular like structures within the left-ventricular scar following coronary artery ligation (Figure S5D). Gli1$^+$ cells from bone chips did not express NG2 in vitro (Figure S2). We then tested whether cultured cells acquire NG2 expression and contribute to neovascularization in an *in vivo* matrigel-plug angiogenesis assay. Four weeks after implantation of Gli1$^+$ cells, we observed developing vessels with Gli1$^+$ cells surrounding CD31$^+$ endothelial cells (Figure S5E). Gli1$^+$ cells adjacent to endothelial cells acquired expression of NG2 and CD146 (Figure S5E).

These experiments suggest that Gli1$^+$ cells acquire expression of NG2 during angiogenesis. Because NG2 can directly bind to PDGF-AA (Goretzki et al., 1999), an essential autocrine regulator of VEGF expression and therefore angiogenesis (Shikada et al., 2005), these results are also consistent with a pro-angiogenic role for NG2 expression in Gli1$^+$ MSC-like cells.

Gli inhibition and myofibroblast differentiation reduces Gli1$^+$ progenitor endothelial cell - tube association *in vitro*

Hh signaling plays a critical role in angiogenesis, while detachment of perivascular cells from capillaries has been proposed as an early event triggering capillary destabilization and hypoxia in fibrosis (Schrimpf et al., 2014). We therefore studied tube formation with Gli1$^+$ cells and endothelial cells (EC) in 3-dimensional collagen gels *in vitro*. Interestingly, Shh treatment increased the number of Gli1$^+$ cells in the gels and promoted their association with EC tubes. Inhibition of Gli1 by GANT61 dramatically reduced the fraction of Gli1$^+$ cells associated with EC-tubes (Figure S6H–K). Our previous data demonstrates that TGF-β treatment leads to myofibroblast differentiation of Gli1$^+$ cells. In the tube formation assays TGF-β significantly reduced the fraction of Gli1$^+$ cells adjacent to EC-tubes, whereas treatment with vascular endothelial growth factor (VEGF-165) resulted in a high fraction of Gli1$^+$ cells associated with EC-tubes. This data suggests that several pathways are important in Gli1$^+$ progenitor – EC-tube association and that myofibroblast differentiation reduces association of Gli1$^+$ cells with EC.

Resident but not circulating Gli1$^+$ progenitor cells contribute to fibrosis

It has been proposed that bone marrow-derived MSC circulate and home to injured kidney where they differentiate into α-SMA$^+$ myofibroblasts (LeBleu et al., 2013). Since our results suggest that Gli1$^+$ cells are myofibroblast progenitors, are MSC-like and that they are located both within organs but also in the bone marrow, we therefore asked whether Gli1$^+$ cells circulate and home to injured organs. While bone marrow transplantation (BMTX) is a standard approach to trace the fate of circulating cells, irradiation injury may promote

fibrosis, alter MSC properties and it is unclear whether MSC actually engraft following BMTX (Cilloni et al., 2000). We therefore utilized both BMTX and also parabiosis, where two mice are conjoined and share one blood circulation, to ask whether Gli1$^+$ cells circulate and home to injured tissue.

Ptprc^a-Pepc^b mice harboring the common leukocyte antigen variant CD45.1 were lethally irradiated and received whole bone marrow of bigenic Gli1CreER^{t2};tdTomato donors (CD45.2) that were injected with tamoxifen prior to sacrifice and BM harvest. Five weeks later, the mice underwent UUO or sham surgery (Figure 6A). Flow cytometric analysis using antibodies specific for the common leukocyte antigen variants demonstrated a successful engraftment of CD45.2$^+$ donor cells into recipient bone marrow (Figure 6B). These engrafted CD45.2$^+$ donor leukocytes migrated into the kidney following UUO surgery, as expected (Figure 6C). However, only a small number of Gli1$^+$ cells engrafted into bone marrow (Figure 6D–E), whereas many more Gli1$^+$ cells were trapped in the lung (Figure 6C–E), consistent with previous reports (Schrepfer et al., 2007). The number of Gli1-tdTomato$^+$ cells between sham, contralateral (CLK) or UUO kidney did not differ significantly and importantly no interstitial tdTomato$^+$ cells were observed (Figure 6D, F). Some Gli1$^+$ cells were also trapped in kidney glomeruli (Figure 6F). Interestingly, Gli1$^+$ cells persisted in the lung at >6 weeks after transplantation, some even expressing α-SMA (Figure 6F). These results suggest that engrafted Gli1$^+$ donor cells do not circulate and home to the kidney nor contribute to the myofibroblast pool following injury (UUO). Since only a small fraction of Gli1$^+$ cells engrafted in bone marrow, however, we next turned to the parabiosis model to examine Gli1$^+$ cell circulation.

Bigenic Gli1CreER^{t2}; tdTomato mice received tamoxifen and were conjoined 10 days after the last tamoxifen injection (Figure 6G). Shared circulation was verified 4 weeks after parabiosis surgery (Figure 6H) and UUO surgery was performed in the Ptprc^a-Pepc^b CD45.1$^+$ parabiont. Mice were sacrificed 10 days later. Flow cytometric analysis of PBS perfused spleens and kidneys showed a complete cross-circulation with CD45.1$^+$ and CD45.2$^+$ leukocytes in the tissue of both mice (Figure 6 I–K). There was a significant influx of CD45.2$^+$ leukocytes from the Gli1CreER^{t2}; tdTomato parabiont in the UUO kidney of the CD45.1$^+$ parabiont (≈17% of all kidney cells, Figure 6J,L), but few Gli1-tdTomato$^+$ cells were detected in CLK or UUO kidney of the CD45.1$^+$ parabiont (Figure 6J, M). Microscopic evaluation failed to detect any Gli1-tdTomato$^+$ cells in the CD45.1$^+$ parabiont despite robust fibrosis and α-SMA positive myofibroblast expansion (Figure 6N). This experiment provides clear evidence that neither circulating nor bone marrow-derived Gli1$^+$ cells contribute to the myofibroblast pool in kidney fibrosis.

Ablation of Gli1$^+$ cells ameliorates kidney fibrosis

To assess the functional contribution of Gli1$^+$ cells to fibrosis, we crossed mice with an inducible human diphtheria toxin receptor allele (iDTR) to Gli1CreER^{t2} mice (Figure 7A). After tamoxife-induced recombination of the transcriptional stop sequence, administration of DTX ablates Gli1$^+$ cells in this model. Tamoxifen was given to bigenic mice before UUO or sham surgery. Following surgery, mice were injected with either DTX or vehicle (PBS) as indicated (Figure 7B). Successful ablation of Gli1$^+$ cells following UUO was verified by

quantitative PCR for DTR mRNA (Figure 7F). There was a striking reduction in kidney fibrosis readouts after DTX compared to vehicle, whereas ablation of the Gli1$^+$ progenitor cell population in the sham group had no appreciable effect (Figures 7C–E, S7A–F). Despite the fact that Gli1$^+$ cells represent only 0.2% of the total PDGFRβ$^+$ kidney cell population, their ablation following injury reduced fibrosis dramatically by ~50% (Figure S7A), indicating that the Gli1$^+$ population plays a critical role regulating fibrosis during chronic injury. To test whether our ablation approach is specific to the Gli1+ population, we generated triple transgenic mice (Gli1CreER^{t2}; iDTR; tdTomato) and repeated the UUO ablation experiment. DTX administration substantially decreased tdTomato$^+$ cells, as expected (Figure S7M–O). We detected apoptotic tdTomato$^+$ cells (TUNEL$^+$) after DTX injection yet we did not observe increased apoptosis in other renal cell populations, providing strong evidence that DTX caused the specific ablation of Gli1$^+$ cells and not other cell types (Figure S7P–Q).

Ablation of Gli1$^+$ cells reduces heart fibrosis and rescues left ventricular function following aortic banding

We next asked whether ablation of Gli1$^+$ cells might improve organ function during chronic disease and utilized the AAC model of heart fibrosis with noninvasive measurement of cardiac function via echocardiography. Gli1CreER^{t2}; iDTR mice were injected with high dose tamoxifen and subjected to AAC or sham surgery. Mice were randomized to receive DTX or vehicle based on their echocardiographically measured peak velocity at the aortic suture site immediately after surgery (Figure S7H) and their left ventricular ejection fraction (EF) at 2 weeks after surgery. DTX or vehicle was given as indicated at 3 and 5 weeks after surgery (Figure 7G).

Ablation of Gli1$^+$ cells after AAC reduced cardiac hypertrophy, heart-weight and cardiomyocyte cross-sectional area (Figure 7G–I). Quantitative PCR confirmed reduction of iDTR mRNA expression by ~75%, indicating successful ablation of Gli1-iDTR$^+$ cells (Figure 7J). Quantification of fibrotic readouts demonstrated a remarkable reduction of interstitial myocardial fibrosis following Gli1$^+$ cell ablation indicating that the perivascular Gli1$^+$ cellpopulation is in fact an important driver of interstitial myocardial fibrosis (Figures 7K–P, S7I–K). Importantly, echocardiographic analysis of left ventricular function demonstrated that ablation of Gli1$^+$ cells rescued chronic heart failure after AAC by preserving left ventricular ejection fraction and thus, myocardial function (Figure 7Q–R). These results indicate that cardiac Gli1$^+$ cells not only drive fibrogenesis in pressure-overload heart failure, but that this process impairs myocardial function.

Discussion

Knowledge concerning the *in vivo* function of MSC in specialized niches such as bone marrow and mouse incisor is growing rapidly (Morrison and Scadden, 2014; Zhao et al., 2014). Thus far however, little is known about the *in vivo* role of MSC in clinically important solid organs such as kidney, heart, lung and liver following injury and during repair. Here we demonstrate that Gli1 expression in adult mice marks a perivascular cell-population that forms an extensive network from the adventitia of large arteries to the

pericyte niche in capillary beds of all major organs tested. These Gli1$^+$ cells express a typical mouse MSC surface profile *in vivo*, are enriched for CFU-F and possess a trilineage differentiation capability *in vitro*, therefore fulfilling the most commonly used definition of what has been termed an MSC (Park et al., 2012). Our data extends the recent finding that Gli1 labels MSClike cells in the mouse incisor (Zhao et al., 2014) and strongly suggests that Gli1 is a general *in vivo* marker for MSC-like cells during adult homeostasis. Indeed, it has become evident in recent years that the perivasculature comprising pericyte and adventitial locus might be the *in vivo* niche of MSC also explaining why MSC can be isolated from virtually all organs (Murray et al., 2014).

Our genetic fate tracing results indicate that resident perivascular Gli1$^+$ cells undergo proliferative expansion following injury and differentiate into myofibroblasts *in vivo.* Indeed, it was noted over a century ago that fibrosis emanates from blood vessels (Atkins, 1875) and recent work implicates vascular pericytes as myofibroblast progenitors in the kidney (Humphreys et al., 2010), lung (Hung et al., 2013), spinal cord (Goritz et al., 2011), dermis and skeletal muscle (Dulauroy et al., 2012). Despite this, the contribution of pericytes to kidney fibrosis has recently been questioned (LeBleu et al., 2013). To date, studies analyzing the role of pericytes in solid organ fibrosis has used broad stromal cell drivers that typically mediate recombination in several different cell types including vascular smooth muscle cells, mesangial cells, resident fibroblasts and pericytes (Asada et al., 2011; Henderson et al., 2013; Humphreys et al., 2010; Hung et al., 2013; LeBleu et al., 2013). A particular strength of our work is that while PDGFRβ is expressed in a relatively large cell population across organs tested, Gli1 specifically labels a very small subset of this cell-population surrounding the macro- and micro-vasculature, which we show is enriched for CFU-F and is committed to the myofibroblast lineage after injury.

The cellular origin of myofibroblasts in cardiac fibrosis has been unclear for many years, although historic observations (Maccallum, 1899) and more recent work have suggested that perivascular cells might be involved (Weber et al., 2013), but no fate tracing data for pericytes or perivascular cells has existed. In fact for many years it was believed that endothelial cells were a major source of myofibroblasts in heart fibrosis via endothelial to mesenchymal transition (EndoMT) (Zeisberg et al., 2007). A very recent paper implicates resident myocardial stroma as the major source of myofibroblasts in pressure overloaded cardiac fibrosis, whereas EndoMT or circulating precursors were not observed (Moore-Morris et al., 2014). These latter results are consistent with our finding that resident perivascular Gli1$^+$ cells with distinct characteristics of MSC differentiate into myofibroblasts following injury of major organs including the heart.

Matrix deposition impairs both systolic and diastolic heart function and myofibroblasts are the main effector cells responsible for this scarring in heart fibrosis. The cardiac interstitium with fibroblasts and extracellular matrix has also been reported to facilitate cardiac hypertrophy (Kakkar and Lee, 2010). However, whether ablation of myofibroblasts can affect scaring, hypertrophy and left ventricular function has remained unclear. Our data clearly demonstrates that ablation of a myofibroblast progenitor population and descendants reduces fibrosis severity, cardiac hypertrophy and rescues systolic left ventricular function following injury. However, our data also suggests that Gli1$^+$ cells might gain markers of

mature pericytes such as NG2 and participate in angiogenesis. Clearly, Gli1$^+$ cells are an intriguing and novel target for heart failure.

MSCs have recently been proposed as a source of scar forming myofibroblasts in heart fibrosis and myelofibrosis by others (Carlson et al., 2011; Schepers et al., 2013). However, this hypothesis has remained speculative due to the absence of genetic fate tracing data. Our results support the idea that tissue resident perivascular MSC-like cells represent a major source of myofibroblasts. They further suggest that under conditions of chronic injury MSC-like cells are not beneficial but actually promote organ fibrosis. This might contradict the hypothesis that MSC act beneficial as “medicinal MSC” that become activated and promote tissue regeneration following injury (Caplan and Correa, 2011) or the fact that exogenous infused MSC promote regeneration or ameliorate progression in many diseases. While fibrotic scar is an adaptive response in certain acute injuries (in myocardial infarction, for example, fibrosis prevents left ventricular rupture), in chronic organ injury progressive myofibroblast expansion with scar deposition is pathologic and ultimately compromises organ function. Our results emphasize that MSC-like cells do not always act in a beneficial way.

Although ablation of Gli1$^+$ cells substantially ameliorated fibrosis in kidney and heart, we observed α-SMA$^+$ myofibroblasts that do not derive from Gli1$^+$ progenitors, suggesting a heterogeneous lineage for the myofibroblast pool. It is striking that Gli1$^+$ cells reflect a very small proportion of total organ cells and even PDGFRβ$^+$ cells, but their ablation reduces fibrosis by ~50% in kidney and heart. Combined with the enhanced clonogenic capacity of Gli1$^+$ cells compared to Gli1$^-$ interstitial cells, these results indicate that Gli1$^+$ MSC-like cells represent a functionally distinct interstitial sub-compartment. The similarity of these cells across organs also implies a conserved response to chronic injury culminating in fibrosis.

The precise identity of myofibroblasts in kidney fibrosis has been a subject of considerable controversy. In contrast with our results here, another recent study reported that neither PDGFRβ nor NG2 expressing cells contribute to the myofibroblast pool in kidney fibrosis (LeBleu et al., 2013). However, early after this report another group demonstrated that PDGFRβ$^+$ cells do indeed contribute to the myofibroblast pool in kidney, lung and heart fibrosis (Henderson et al., 2013). That myofibroblasts express PDGFRβ$^+$ has been known for many years (Asada et al., 2011; Humphreys et al., 2010; Kramann et al., 2013). While the reasons for these discrepant results are unclear, mosaic transgene expression or expression patterns unfaithful to the endogenous allele, both known properties of random integration transgenics, is one possible explanation (Duffield, 2014; Le et al., 2006). Our results here clearly indicate that all myofibroblasts express PDGFRβ and that Gli1$^+$ cells do not acquire significant NG2 expression in classical fibrosis models.

The contribution of circulating, bone marrow derived progenitor cells to the pool of myofibroblasts is also controversial (Kramann et al., 2013) and some evidence suggests that bone marrow-derived MSC enter the circulation and home to sites of injury. Our data from BMTX and parabiosis approaches provide conclusive evidence that Gli1$^+$ MSC-like cells

are tissue resident cells that do not arise from the circulation. However, we cannot exclude a contribution from $Gli1^-$ circulating cells.

Most studies of Hh signaling during fibrosis suggest that Hh ligands Shh and Ihh drive myofibroblast proliferation and activation (Fabian et al., 2012; Michelotti et al., 2013). However, Hh signaling is also critical in angiogenesis and Shh gene transfer has been shown to reduce fibrosis and conserve left ventricular function following myocardial ischemia, possibly reflecting Shh driven pro-angiogenic signaling in the heart (Kusano et al., 2005). Consistent with this possibility, we found that both Shh and VEGF increased the number of $Gli1^+$ cells associated with EC tubes. Shh also mediates pro-angiogenic signaling by upregulating VEGF expression (Pola et al., 2003; Pola et al., 2001) and VEGF can induce expression of the hedgehog transcriptional activator Gli1 (Goel and Mercurio, 2013), suggesting the possible existence of a positive feedback loop.

Our data suggest dual roles for $Gli1^+$ cells in both fibrosis and angiogenesis. Gli1 is a transcriptional readout of Hh pathway activity indicating that $Gli1^+$ MSC-like cells respond to Hh ligand. Consistent with this, nerve-derived Shh drives of Gli1 in mouse incisor MSC (Zhao et al., 2014) and a similar paradigm has been described for the hair follicle (Brownell et al., 2011). Whether or not such a paracrine signaling loop exists for organ resident MSC-like cells is unclear. We analyzed bigenic $ShhCreER^{t2+}$, $tdTomato^+$ mice for expression of Shh-positive cells in adult mice, and we did not observe any $tdTomato^+$ cells in kidney or heart up to 2 weeks after tamoxifen injection or after injury (data not shown). The known roles for Gli1 in regulating cell proliferation and self-renewal of stem cells suggest similar roles in MSC-like cells (Merchant et al., 2010; Takanaga et al., 2009). Indeed, our data points toward constitutive expression of Gli1 in $Gli1^+$ MSC-like cells *in vitro*, while inhibition of Gli by GANT61 reduces both self-renewal and association of $Gli1^+$ cells with endothelial tubes. Whether steady state Gli expression might promote a quiescent state of perivascular $Gli1^+$ cells will require further investigation.

Experimental procedures

Mice

All mouse experiments were performed according to the animal experimental guidelines issued by the Animal Care and Use Committee at Harvard University. Gli1-nLacZ (JAX #008211) $Gli1CreER^{t2}$ (JAX #007913), Rosa26tdTomato (JAX #007909) iDTR mice (JAX # 007900), $Ptprc^a$-$Pepc^b$ mice (JAX #002014) were purchased from Jackson Laboratories (Bar Harbor, ME). For lineage tracing studies 6–7 week old mice received 3 × 0.1mg/kg bodyweight tamoxifen in corn oil / 3% ethanol (Sigma) via intraperitoneal injection 10days before surgery or disease induction unless otherwise stated. All models of organ injury and cell-specific ablation experiments are described in the Supplementary Experimental Procedures.

Bone marrow transplantation experiments

The whole bone marrow was harvested from Gli1CreERt2; tdTomato mice (CD45.2) that had received tamoxifen injection previously. 2×10^6 FACS sorted Gli1-tdTomato+ cells

isolated from bone chips of bigenic Gli1CreERt2,tdTomato mice were added to 3×10^6 freshly isolated whole bone marrow cells per recipient and injected into the tail-vein of lethally irradiated (1050 Rads) CD45.1 positive recipient mice (JAX #002014).

Parabiosis

Bigenic Gli1CreER^{t2}; tdTomato mice (8 week old) received tamoxifen (3 × 0.4 mg/kg bodyweight by gavage) and were conjoined to wildtype CD45.1 mice (JAX #002014, 8 week old) 10 days after the last tamoxifen injection. Parabiosis was performed as previously described (Ruckh et al., 2012). Cross circulation was confirmed by flow cytometry of peripheral blood, splenocytes and digested kidneys using antibodies specific for the common leukocyte variants CD45.1 and CD45.2.

Gene / Protein expression

Primers are described in Table S1, antibodies and methods are described in the Supplementary Experimental Procedures.

Echocardiography

Echocardiography was performed in the AAC cell-ablation experiment immediately following the AAC surgery to determine the peak velocity at the constriction, 2 weeks after surgery before the randomization to DTX or Vehicle group and at 4 and 8 weeks after the surgery in low dose isoflurane anesthesia (1.5%) using a 28MHz linear array transducer connected to a digital ultrasound console (Vevo 2100 Visualsonics). Images and loops were stored and analyzed offline using the Vevo 2100 analysis software (1.6.0 Visualsonics).

Supplementary Material

Refer to Web version on PubMed Central for supplementary material.

Acknowledgements

This work was supported by NIH/NIDDK (DK088923 and DK103050), the NIDDK Diabetic Complications Consortium (DK076169), by the Harvard Stem Cell Institute and by an Established Investigator Award of the American Heart Association (all to BDH) and by a fellowship from the Deutsche Forschungsgemeinschaft (to RK Kr 40731-1 and RKS Schn 1188/3-1). We thank Sudeshna Fisch and Soeun Ngoy from the cardiovascular core of the Brigham and Women´s Hospital for technical support.

References

Asada N, Takase M, Nakamura J, Oguchi A, Asada M, Suzuki N, Yamamura K, Nagoshi N, Shibata S, Rao TN, et al. Dysfunction of fibroblasts of extrarenal origin underlies renal fibrosis and renal anemia in mice. The Journal of clinical investigation. 2011; 121:3981–3990. [PubMed: 21911936]

Atkins R. On Arterio-Capillary Fibrosis. British medical journal. 1875; 1:444–446.

Boxall SA, Jones E. Markers for characterization of bone marrow multipotential stromal cells. Stem cells international. 2012; 2012:975871. [PubMed: 22666272]

Brownell I, Guevara E, Bai CB, Loomis CA, Joyner AL. Nerve-derived sonic hedgehog defines a niche for hair follicle stem cells capable of becoming epidermal stem cells. Cell stem cell. 2011; 8:552–565. [PubMed: 21549329]

Caplan AI. Mesenchymal stem cells. Journal of orthopaedic research : official publication of the Orthopaedic Research Society. 1991; 9:641–650. [PubMed: 1870029]

Caplan AI, Correa D. The MSC: an injury drugstore. Cell stem cell. 2011; 9:11–15. [PubMed: 21726829]

Carlson S, Trial J, Soeller C, Entman ML. Cardiac mesenchymal stem cells contribute to scar formation after myocardial infarction. Cardiovascular research. 2011; 91:99–107. [PubMed: 21357194]

Cilloni D, Carlo-Stella C, Falzetti F, Sammarelli G, Regazzi E, Colla S, Rizzoli V, Aversa F, Martelli MF, Tabilio A. Limited engraftment capacity of bone marrow-derived mesenchymal cells following T-cell-depleted hematopoietic stem cell transplantation. Blood. 2000; 96:3637–3643. [PubMed: 11071665]

Crisan M, Yap S, Casteilla L, Chen CW, Corselli M, Park TS, Andriolo G, Sun B, Zheng B, Zhang L, et al. A perivascular origin for mesenchymal stem cells in multiple human organs. Cell stem cell. 2008; 3:301–313. [PubMed: 18786417]

Danis A. Study of ossification in bone marrow grafts. Acta chirurgica Belgica. 1957; 56:1–120. [PubMed: 13582484]

Duffield JS. Cellular and molecular mechanisms in kidney fibrosis. The Journal of clinical investigation. 2014; 124:2299–2306. [PubMed: 24892703]

Dulauroy S, Di Carlo SE, Langa F, Eberl G, Peduto L. Lineage tracing and genetic ablation of ADAM12(+) perivascular cells identify a major source of profibrotic cells during acute tissue injury. Nature medicine. 2012; 18:1262–1270.

Fabian SL, Penchev RR, St-Jacques B, Rao AN, Sipila P, West KA, McMahon AP, Humphreys BD. Hedgehog-Gli pathway activation during kidney fibrosis. Am J Pathol. 2012; 180:1441–1453. [PubMed: 22342522]

Fukushi J, Makagiansar IT, Stallcup WB. NG2 proteoglycan promotes endothelial cell motility and angiogenesis via engagement of galectin-3 and alpha3beta1 integrin. Molecular biology of the cell. 2004; 15:3580–3590. [PubMed: 15181153]

Goel HL, Mercurio AM. VEGF targets the tumour cell. Nature reviews Cancer. 2013; 13:871–882.

Goretzki L, Burg MA, Grako KA, Stallcup WB. High-affinity binding of basic fibroblast growth factor and platelet-derived growth factor-AA to the core protein of the NG2 proteoglycan. The Journal of biological chemistry. 1999; 274:16831–16837. [PubMed: 10358027]

Goritz C, Dias DO, Tomilin N, Barbacid M, Shupliakov O, Frisen J. A pericyte origin of spinal cord scar tissue. Science. 2011; 333:238–242. [PubMed: 21737741]

Henderson NC, Arnold TD, Katamura Y, Giacomini MM, Rodriguez JD, McCarty JH, Pellicoro A, Raschperger E, Betsholtz C, Ruminski PG, et al. Targeting of alphav integrin identifies a core molecular pathway that regulates fibrosis in several organs. Nature medicine. 2013; 19:1617–1624.

Humphreys BD, Lin SL, Kobayashi A, Hudson TE, Nowlin BT, Bonventre JV, Valerius MT, McMahon AP, Duffield JS. Fate tracing reveals the pericyte and not epithelial origin of myofibroblasts in kidney fibrosis. Am J Pathol. 2010; 176:85–97. [PubMed: 20008127]

Hung C, Linn G, Chow YH, Kobayashi A, Mittelsteadt K, Altemeier WA, Gharib SA, Schnapp LM, Duffield JS. Role of lung pericytes and resident fibroblasts in the pathogenesis of pulmonary fibrosis. American journal of respiratory and critical care medicine. 2013; 188:820–830. [PubMed: 23924232]

Kakkar R, Lee RT. Intramyocardial fibroblast myocyte communication. Circulation research. 2010; 106:47–57. [PubMed: 20056945]

Kramann R, DiRocco DP, Humphreys BD. Understanding the origin, activation and regulation of matrix-producing myofibroblasts for treatment of fibrotic disease. The Journal of pathology. 2013; 231:273–289. [PubMed: 24006178]

Kramann R, Tanaka M, Humphreys BD. Fluorescence Microangiography for Quantitative Assessment of Peritubular Capillary Changes after AKI in Mice. Journal of the American Society of Nephrology : JASN. 2014; 25:1924–1931. [PubMed: 24652794]

Kusano KF, Pola R, Murayama T, Curry C, Kawamoto A, Iwakura A, Shintani S, Ii M, Asai J, Tkebuchava T, et al. Sonic hedgehog myocardial gene therapy: tissue repair through transient reconstitution of embryonic signaling. Nature medicine. 2005; 11:1197–1204.

Le YZ, Zheng L, Zheng W, Ash JD, Agbaga MP, Zhu M, Anderson RE. Mouse opsin promoter-directed Cre recombinase expression in transgenic mice. Molecular vision. 2006; 12:389–398. [PubMed: 16636658]

LeBleu VS, Taduri G, O'Connell J, Teng Y, Cooke VG, Woda C, Sugimoto H, Kalluri R. Origin and function of myofibroblasts in kidney fibrosis. Nature medicine. 2013; 19:1047–1053.

Maccallum JB. A Contribution to the Knowledge of the Pathology of Fragmentation and Segmentation, and Fibrosis of the Myocardium. The Journal of experimental medicine. 1899; 4:409–424.

Merchant A, Joseph G, Wang Q, Brennan S, Matsui W. Gli1 regulates the proliferation and differentiation of HSCs and myeloid progenitors. Blood. 2010; 115:2391–2396. [PubMed: 20107231]

Michelotti GA, Xie G, Swiderska M, Choi SS, Karaca G, Kruger L, Premont R, Yang L, Syn WK, Metzger D, et al. Smoothened is a master regulator of adult liver repair. The Journal of clinical investigation. 2013; 123:2380–2394. [PubMed: 23563311]

Moore-Morris T, Guimaraes-Camboa N, Banerjee I, Zambon AC, Kisseleva T, Velayoudon A, Stallcup WB, Gu Y, Dalton ND, Cedenilla M, et al. Resident fibroblast lineages mediate pressure overload-induced cardiac fibrosis. The Journal of clinical investigation. 2014; 124:2921–2934. [PubMed: 24937432]

Morrison SJ, Scadden DT. The bone marrow niche for haematopoietic stem cells. Nature. 2014; 505:327–334. [PubMed: 24429631]

Murfee WL, Rehorn MR, Peirce SM, Skalak TC. Perivascular cells along venules upregulate NG2 expression during microvascular remodeling. Microcirculation. 2006; 13:261–273. [PubMed: 16627368]

Murray IR, West CC, Hardy WR, James AW, Park TS, Nguyen A, Tawonsawatruk T, Lazzari L, Soo C, Peault B. Natural history of mesenchymal stem cells, from vessel walls to culture vessels. Cellular and molecular life sciences : CMLS. 2014; 71:1353–1374. [PubMed: 24158496]

Park D, Spencer JA, Koh BI, Kobayashi T, Fujisaki J, Clemens TL, Lin CP, Kronenberg HM, Scadden DT. Endogenous bone marrow MSCs are dynamic, fate-restricted participants in bone maintenance and regeneration. Cell stem cell. 2012; 10:259–272. [PubMed: 22385654]

Pelekanos RA, Li J, Gongora M, Chandrakanthan V, Scown J, Suhaimi N, Brooke G, Christensen ME, Doan T, Rice AM, et al. Comprehensive transcriptome and immunophenotype analysis of renal and cardiac MSC-like populations supports strong congruence with bone marrow MSC despite maintenance of distinct identities. Stem cell research. 2012; 8:58–73. [PubMed: 22099021]

Pola R, Ling LE, Aprahamian TR, Barban E, Bosch-Marce M, Curry C, Corbley M, Kearney M, Isner JM, Losordo DW. Postnatal recapitulation of embryonic hedgehog pathway in response to skeletal muscle ischemia. Circulation. 2003; 108:479–485. [PubMed: 12860919]

Pola R, Ling LE, Silver M, Corbley MJ, Kearney M, Blake Pepinsky R, Shapiro R, Taylor FR, Baker DP, Asahara T, et al. The morphogen Sonic hedgehog is an indirect angiogenic agent upregulating two families of angiogenic growth factors. Nature medicine. 2001; 7:706–711.

Ruckh JM, Zhao JW, Shadrach JL, van Wijngaarden P, Rao TN, Wagers AJ, Franklin RJ. Rejuvenation of regeneration in the aging central nervous system. Cell stem cell. 2012; 10:96–103. [PubMed: 22226359]

Schepers K, Pietras EM, Reynaud D, Flach J, Binnewies M, Garg T, Wagers AJ, Hsiao EC, Passegue E. Myeloproliferative neoplasia remodels the endosteal bone marrow niche into a self-reinforcing leukemic niche. Cell stem cell. 2013; 13:285–299. [PubMed: 23850243]

Schrepfer S, Deuse T, Reichenspurner H, Fischbein MP, Robbins RC, Pelletier MP. Stem cell transplantation: the lung barrier. Transplantation proceedings. 2007; 39:573–576. [PubMed: 17362785]

Schrimpf C, Teebken OE, Wilhelmi M, Duffield JS. The Role of Pericyte Detachment in Vascular Rarefaction. Journal of vascular research. 2014; 51:247–258. [PubMed: 25195856]

Shikada Y, Yonemitsu Y, Koga T, Onimaru M, Nakano T, Okano S, Sata S, Nakagawa K, Yoshino I, Maehara Y, et al. Platelet-derived growth factor-AA is an essential and autocrine regulator of vascular endothelial growth factor expression in non-small cell lung carcinomas. Cancer research. 2005; 65:7241–7248. [PubMed: 16103075]

Song S, Ewald AJ, Stallcup W, Werb Z, Bergers G. PDGFRbeta+ perivascular progenitor cells in tumours regulate pericyte differentiation and vascular survival. Nature cell biology. 2005; 7:870–879.

Stallcup WB. The NG2 proteoglycan: past insights and future prospects. Journal of neurocytology. 2002; 31:423–435. [PubMed: 14501214]

Stark K, Eckart A, Haidari S, Tirniceriu A, Lorenz M, von Bruhl ML, Gartner F, Khandoga AG, Legate KR, Pless R, et al. Capillary and arteriolar pericytes attract innate leukocytes exiting through venules and 'instruct' them with pattern-recognition and motility programs. Nature immunology. 2013; 14:41–51. [PubMed: 23179077]

Takanaga H, Tsuchida-Straeten N, Nishide K, Watanabe A, Aburatani H, Kondo T. Gli2 is a novel regulator of sox2 expression in telencephalic neuroepithelial cells. Stem cells. 2009; 27:165–174. [PubMed: 18927476]

Weber KT, Sun Y, Bhattacharya SK, Ahokas RA, Gerling IC. Myofibroblast-mediated mechanisms of pathological remodelling of the heart. Nature reviews Cardiology. 2013; 10:15–26.

Weber KT, Sun Y, Guarda E, Katwa LC, Ratajska A, Cleutjens JP, Zhou G. Myocardial fibrosis in hypertensive heart disease: an overview of potential regulatory mechanisms. European heart journal. 1995; 16(Suppl C):24–28. [PubMed: 7556268]

Zeisberg EM, Tarnavski O, Zeisberg M, Dorfman AL, McMullen JR, Gustafsson E, Chandraker A, Yuan X, Pu WT, Roberts AB, et al. Endothelial-to-mesenchymal transition contributes to cardiac fibrosis. Nature medicine. 2007; 13:952–961.

Zhao H, Feng J, Seidel K, Shi S, Klein O, Sharpe P, Chai Y. Secretion of shh by a neurovascular bundle niche supports mesenchymal stem cell homeostasis in the adult mouse incisor. Cell stem cell. 2014; 14:160–173. [PubMed: 24506883]

Significance

The cellular origin of fibrosis is controversial across different tissues and disciplines and it remains unknown whether a common myofibroblast progenitor cell exists. Here we demonstrate that Gli1 marks a network of perivascular progenitor cells with distinct characteristics of mesenchymal stem cells. Upon injury of liver, lung, kidney or heart, these $Gli1^+$ cells differentiate into myofibroblasts and genetic ablation of these $Gli1^+$ cells ameliorates fibrosis and rescues organ function. Our data indicates that $Gli1^+$ cells represent a minority of the mesenchymal PDGFR-β^+ pool but are committed to fibrosis following injury across organs and therefore they represent a novel therapeutic target.

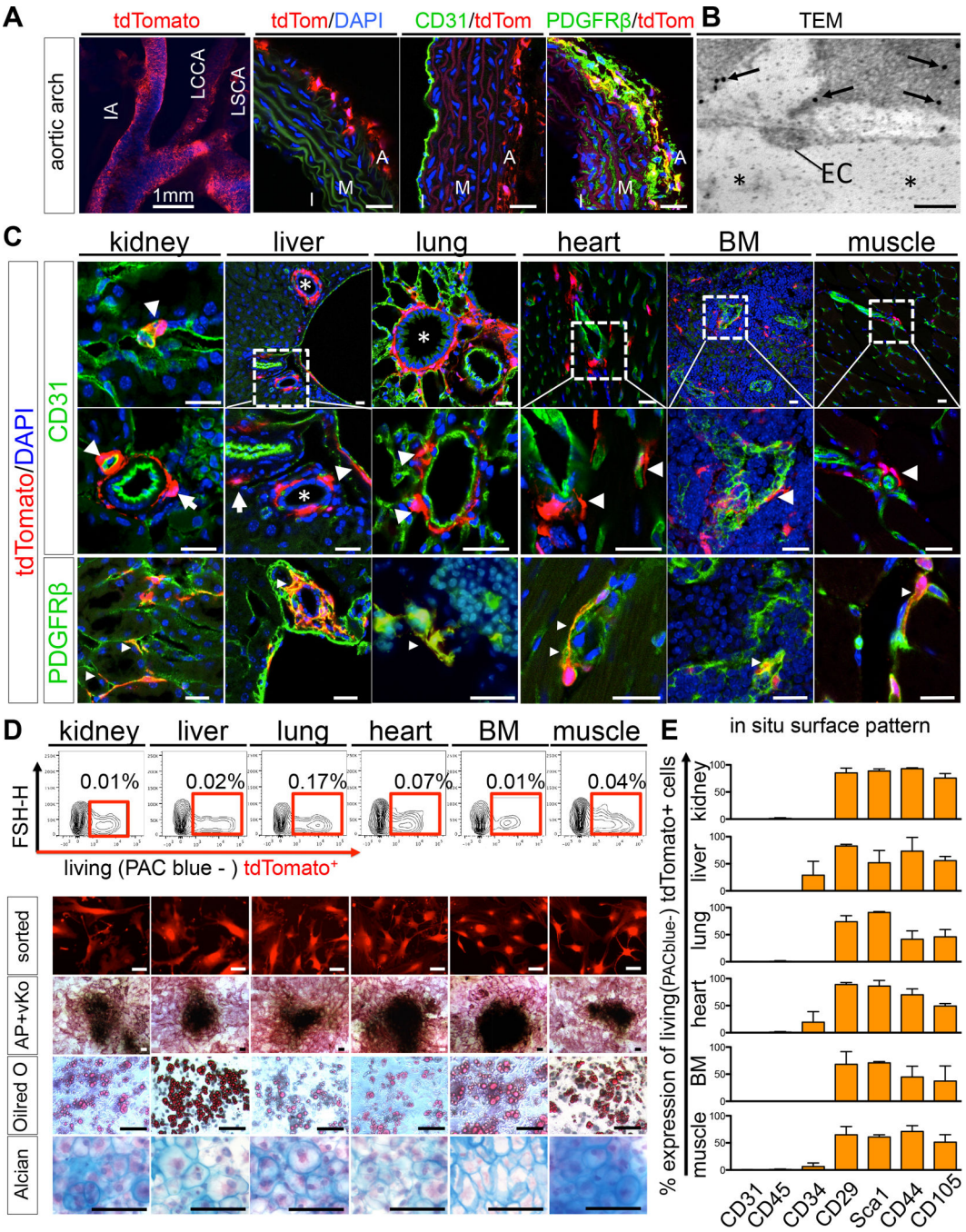

Figure 1. Gli1 defines a perivascular MSC-like cell population residing as adventitial progenitors and in the pericyte niche

(A) Adult Gli1Cre-ER^{t2}; tdTomato mice 48h after tamoxifen administration. Aortic root with innominate artery (IA), left common carotid artery (LCCA) and left subclavian artery (LSCA). Gli1^{+} cells reside in the adventitia (A) distant from CD31^{+} endothelial cells of the intima (I) and media (M) and are PDGFR-β^{+}. Scale bars 20μm or as indicated.

(**B–C**) Gli1-tdTomato^{+} cells also reside adjacent to CD31^{+} endothelial cells across organs tested (EC in B and arrowheads in C). Transmission electron microscopy (TEM) picture of

immunogold labeled (arrows in B) Gli1$^+$ interstitial kidney cell adjacent to an endothelial cell (EC, asterisk in B capillary lumen). Gli1$^+$ cells are PDGFR-β+ (small arrowheads in C). Gli1-tdTomato$^+$ are located around biliary ducts (asterisk liver) and pulmonary bronchi and bronchioles (asterisk lung). Scale bars: 0.2μm in B and 20μm in C.

(**D**) Sorted Gli1-tdTomato$^+$ cells possess *in vitro* trilineage differentiation capacity towards osteoblasts (alkaline phosphatase-AP + von Kossa-vKo staining), adipocytes (Oilred O staining) and chrondrocytes (Alcian Blue staining, experiments were repeated at least 3 times, Scale bars all 50μm, AP+vKo 100μm).

(**E**) Flow cytometry of whole organs demonstrates a typical MSC surface pattern of Gli1-tdTomato$^+$ cells. Data is presented as mean ± SEM, n=3, see also figure S1.

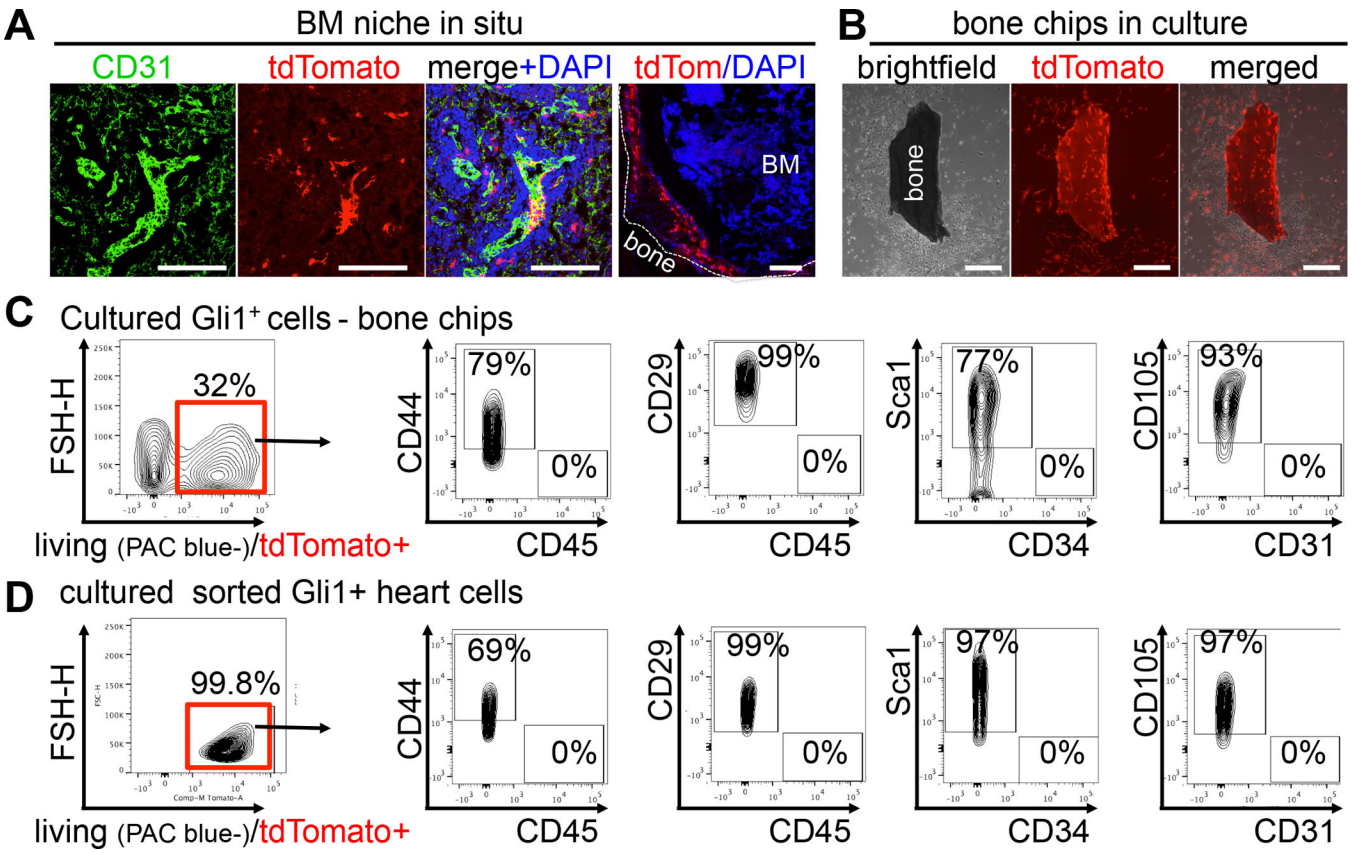

Figure 2. Gli1^{+} cells reside in a typical MSC niche of the bone-marrow and retain their typical MSC-like surface pattern in culture

(A) Gli1-tdTomato^{+} cells surrounding endothelial cells of bone marrow sinusoids and along the endosteum. Scale bars 100μm.

(B) Gli1^{+} cells migrating out of compact bone chips in vitro. Scale bars 200μm.

(C) Flow cytometry of BM-MSC isolated from compact bone chips of Gli1CreER^{t2}; tdTomato mice after 4 weeks of culture indicating that 32% of the cells are of Gli1^{+} origin (tdTomato^{+}) and maintain a typical mouse MSC surface profile.

(D) Flow cytometry of cultured (4 weeks) Gli1^{+}tdTomato^{+} cells from the myocardium with a similar surface profile. Data represents at least 3 independent experiments, see also figure S2.

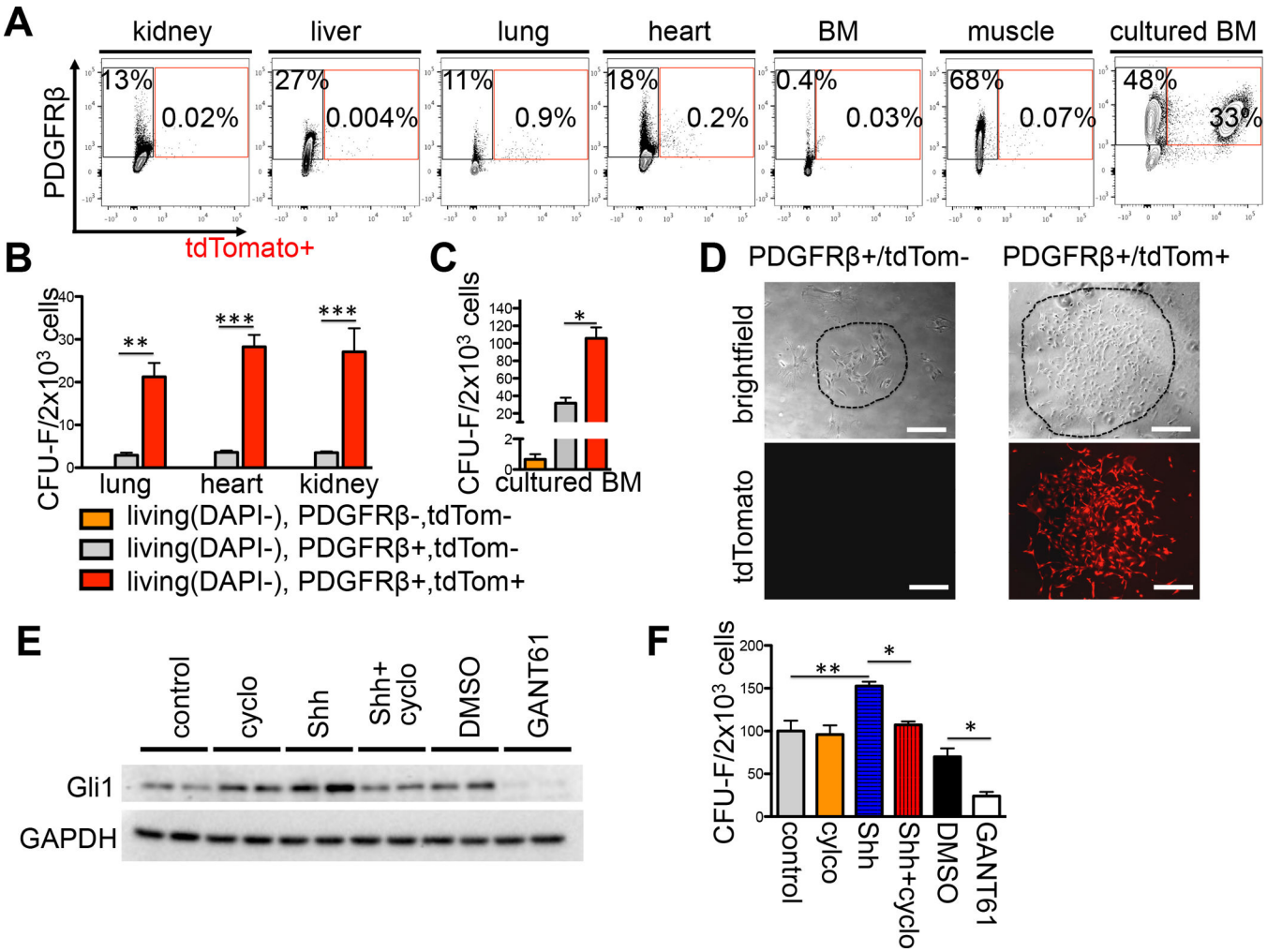

Figure 3. Gli1$^+$ cells represent a small CFU-F enriched fraction of the PDGFRβ$^+$ population while inhibition of Gli reduces their self-renewal

(A) Gli1-tdTomato$^+$ cells represent only a small fraction of the PDGFRβ$^+$ kidney cell population.

(B) PDGFRβ$^+$, Gli1tdTomato+ cells exhibit superior clonogenicity by CFU-F assay (>50 cells/colony at 14 days, n = 3, *p < 0.05 by t-test, mean ± SEM).

(C) Gli1tdTomato$^+$ cells from cultured bone chip also exhibit superior clonogenicity by CFU-F assay.

(D) Colonies cultured from whole hearts 7 days after sorting.

(E) Gli1 protein level is regulated by the hedgehog pathway in Gli1$^+$ cells cultured from bone chips.

(F) Hedgehog pathway also regulates clonogenicicty of Gli1$^+$ cells cultured from bone chips. (cyclo, cyclopamine; Shh, sonic hedgehog). Scale bars 500μm, *p<0.05 **p<0.01, ***p<0.001 by t-test, mean ± SEM, see also figure S3.

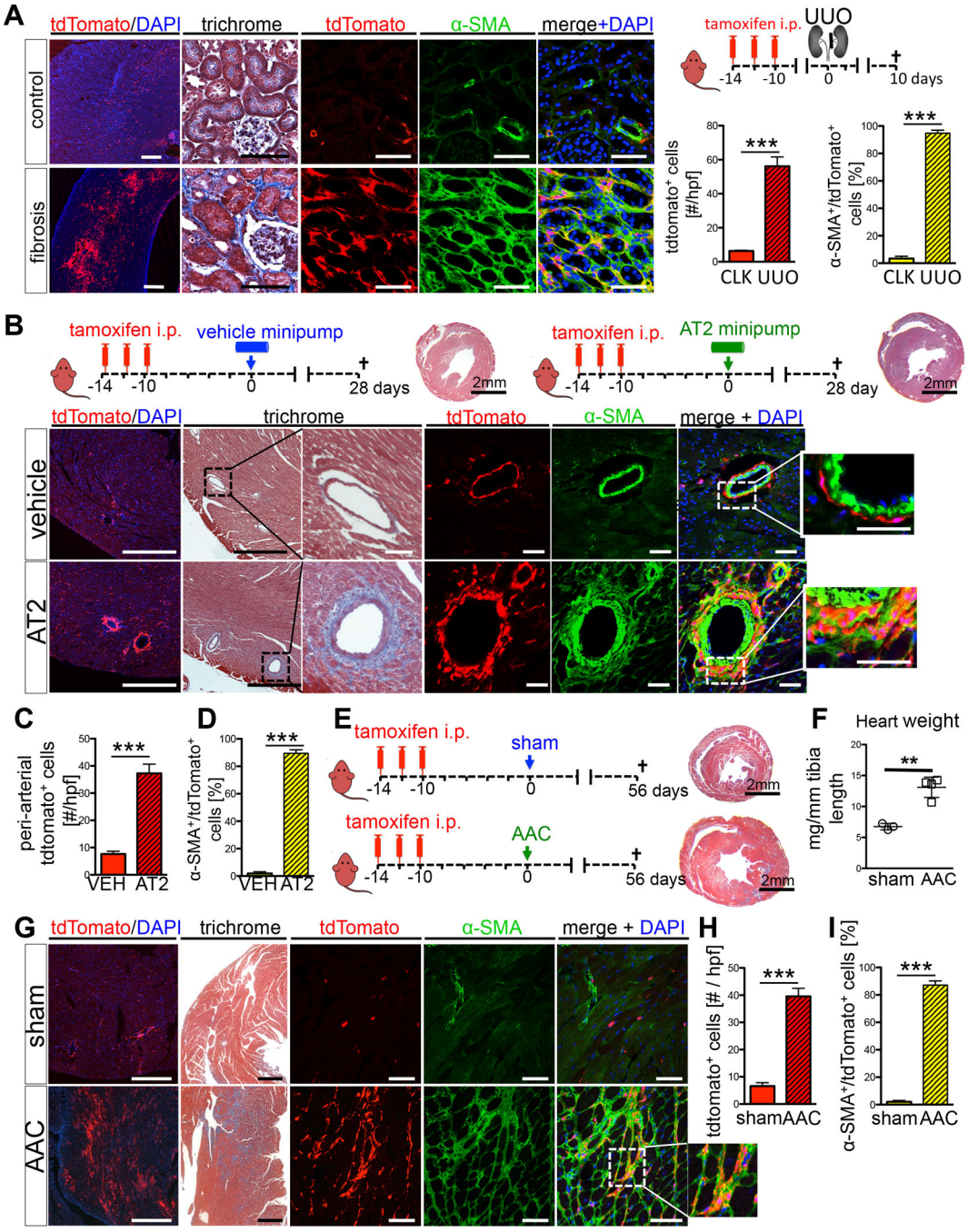

Figure 4. Following kidney or heart injury Gli1$^+$ cells expand and differentiate into myofibroblasts

(**A**) Genetic lineage analysis of Gli1$^+$ cells after unilateral ureteral obstruction (UUO, n=4). Gli1$^+$ cells expand after UUO and acquire alpha smooth muscle actin (α-SMA) expression. tdTomato or α-SMA increase measured in 400× high power fields (hpf). Scale bars: left panel 500μm, all others 50μm; ***p<0.001 by t-test, mean ± SEM.

(**B**–**D**) Myocardial fibrosis induced by angiotensin 2 (AT2, n=4; PBS, n=3) causes hypertension induced, predominantly perivascular fibrosis around myocardial arteries where

Gli1$^+$ cells expand and differentiate into α-SMA$^+$ myofibroblasts. Quantification by confocal micrographs in 400× hpf. Scale bars: left two panels 500μm, all others 50μm; ***p<0.001 by t-test, mean ± SEM.

(**E**–**I**) Ascending aortic constriction induces cardiac hypertrophy, fibrosis and chronic heart failure (AAC, n=4; sham n=3). Following AAC, Gli1$^+$ cells expand dramatically in the myocardial interstitium and acquire α-SMA expression. Quantification by confocal micrographs in 400× hpf. For studying co-expression of tdTomato and α-SMA it is important to study the perinuclear region due to a converse α-SMA tdTomato expression pattern (see figure S4G). Scale bars: left two panels 500μm, all others 50μm; **p<0.05, ***p<0.001 by t-test, mean ± SEM, see also figures S4–5.

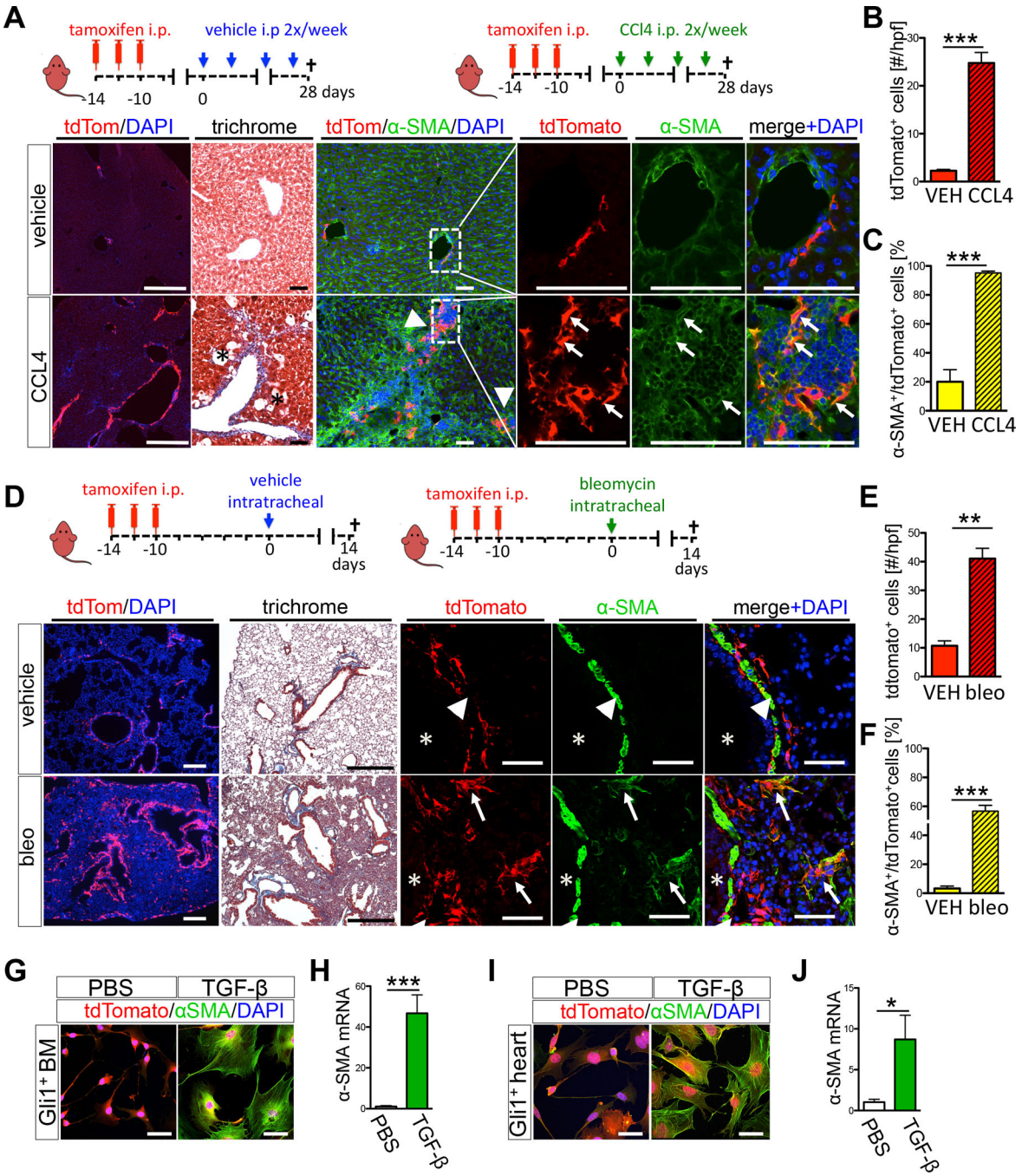

Figure 5. Fate tracing of Gli1$^+$ cells in liver and lung injury

(A–C) Hepatic fibrosis was induced by carbon tetrachloride injections (CCL4, n=5; vehicle, n=3) twice per week and the fate of Gli1-labeled cells analyzed. Hepatocyte necrosis (asterisk) and fibrosis was visible, with expansion of Gli1$^+$tdTomato$^+$ cells in fibrotic areas (arrowheads). Gli1$^+$ cells acquired α-SMA expression (arrows). Throughout figure, quantification was from confocal micrographs in 400× hpf, in this case from periportal and pericentral fields in B and C. Scale bars: left panel 500μm, all others 50μm, ***p<0.001 by t-test, mean ± SEM.

(D–F) Pulmonary fibrosis was induced by bleomycin (n=4) or vehicle (n=3). Low magnification (left panel) shows $Gli1^+$ expansion (quantification in E) with severe pulmonary fibrosis (trichrome). $Gli1^+$ cells line the peri-bronchial smooth muscle cell layer (arrowhead, bronchuslumen = asterisk) of a healthy non-injured lung. In fibrosis $Gli1^+$ cells expand into interstitium and acquire α-SMA expression (arrows, quantification in (F). Scale bars: left two panels 500μm, all others 20μm; **=p<0.01, ***=p<0.001 by t-test, mean ±SEM

(**G–J**) Sorted $Gli1^+$ cells compact bone or myocardium differentiate into $\alpha\text{-SMA}^+$ myofibroblasts after exposure (24h) to transforming growth factor beta (TGF-β) *in vitro* (n=3). Scale bars: 50μm; *p<0.05, ***p<0.001 by t-test, mean±SEM, see also figure S4–5.

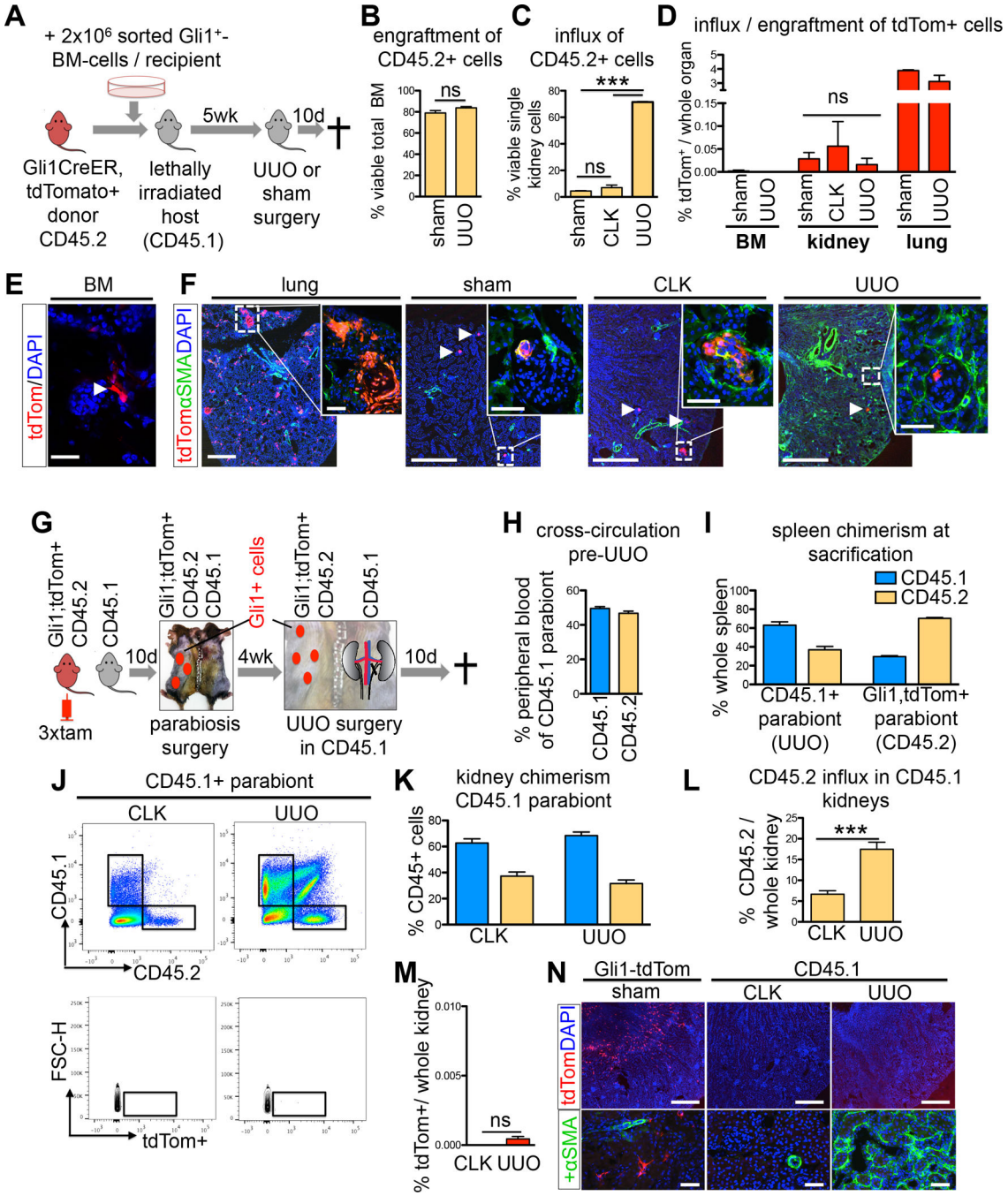

Figure 6. Circulating Gli1$^+$ cells do not contribute to kidney fibrosis

(A) Bone marrow transplantation scheme. Marrow from genetically labeled Gli1CreER^{t2}, tdTomato donors was transplanted into lethally irradiated, unlabeled CD45.1 recipients. 2×10^6 sorted Gli1$^+$ cells from bone chips was added to the whole bone-marrow cell-solution to increase the number of transplanted Gli1$^+$ cells. After verifying engraftment, recipients underwent 5 UUO (n = 5) or sham (n = 3) surgery.

(B) Verification of engraftment of CD45.2$^+$ donor leukocytes into CD45.1 recipients.

(C) CD45.2$^+$ leukocytes from Gli1CreER^{t2}, tdTomato donor increase in UUO kidney of the CD45.1$^+$ recipient compared to the contralateral (CLK) or sham kidney. Data assessed by flow cytometry of whole digested kidneys. (n=3 sham, n=5 CLK, n=5 UUO). ***p<0.001 by one way ANOVA with posthoc Tukey.

(D) No increase in tdTomato$^+$ cells in recipients kidneys 10 days after UUO (n=3 sham, n=5 CLK, n=5 UUO). P = NS by one way ANOVA with posthoc Tukey.

(E–F) tdTomato$^+$ cell distribution in bone marrow (BM), lung, sham-, contralateral- (CLK) and UUO kidneys of recipients. Scale bars 25μm left panel all others 500μm, inserts 50μm.

(G–H) Parabiosis experimental design. After tamoxifen, Gli1CreER^{t2}; tdTomato mice (CD45.2$^+$) were conjoined with unlabeled (CD45.1$^+$) mice. Shared circulation was verified by flow cytometric analysis of peripheral blood from the CD45.1$^+$ parabiont (H, n=8). Thereafter UUO was performed in the CD45.1$^+$ parabiont and analyzed 10 days after surgery.

(I) Spleen chimerism for the common leukocyte antigen variants assessed by flow cytometry (n=8 pairs, mean±SEM).

(J) Flow cytometric plots of whole digested CLK and UUO kidney from the CD45.1$^+$ parabiont indicating influx of leukocytes from the Gli1-tdTomato parabiont with almost no detection of tdTomato$^+$.

(K) Chimerism for CD45.1$^+$ versus CD45.2$^+$ leukocytes in CLK and UUO kidneys (n=8, mean±SEM).

(L) Influx of CD45.2$^+$ leukocytes from the Gli1-tdTomato parabiont in CLK and UUO kidneys (n=8, ***p<0.001 by t-test, mean±SEM).

(M) Gli1-tdTomato cells do not circulate. Almost no tdTomato$^+$ cells are detected in the kidneys of the CD45.1 (n=8; p = NS by t-teat, mean ± SEM).

(N) Gli1-tdTomato$^+$ cells are seen in the uninjured kidneys of the CD45.2 parabiont, however no Gli1-tdTomato$^+$ cells are observed in the CD45.1 parabiont despite robust fibrosis (αSMA staining). Scale bars: top panel 500μm, bottom 50μm.

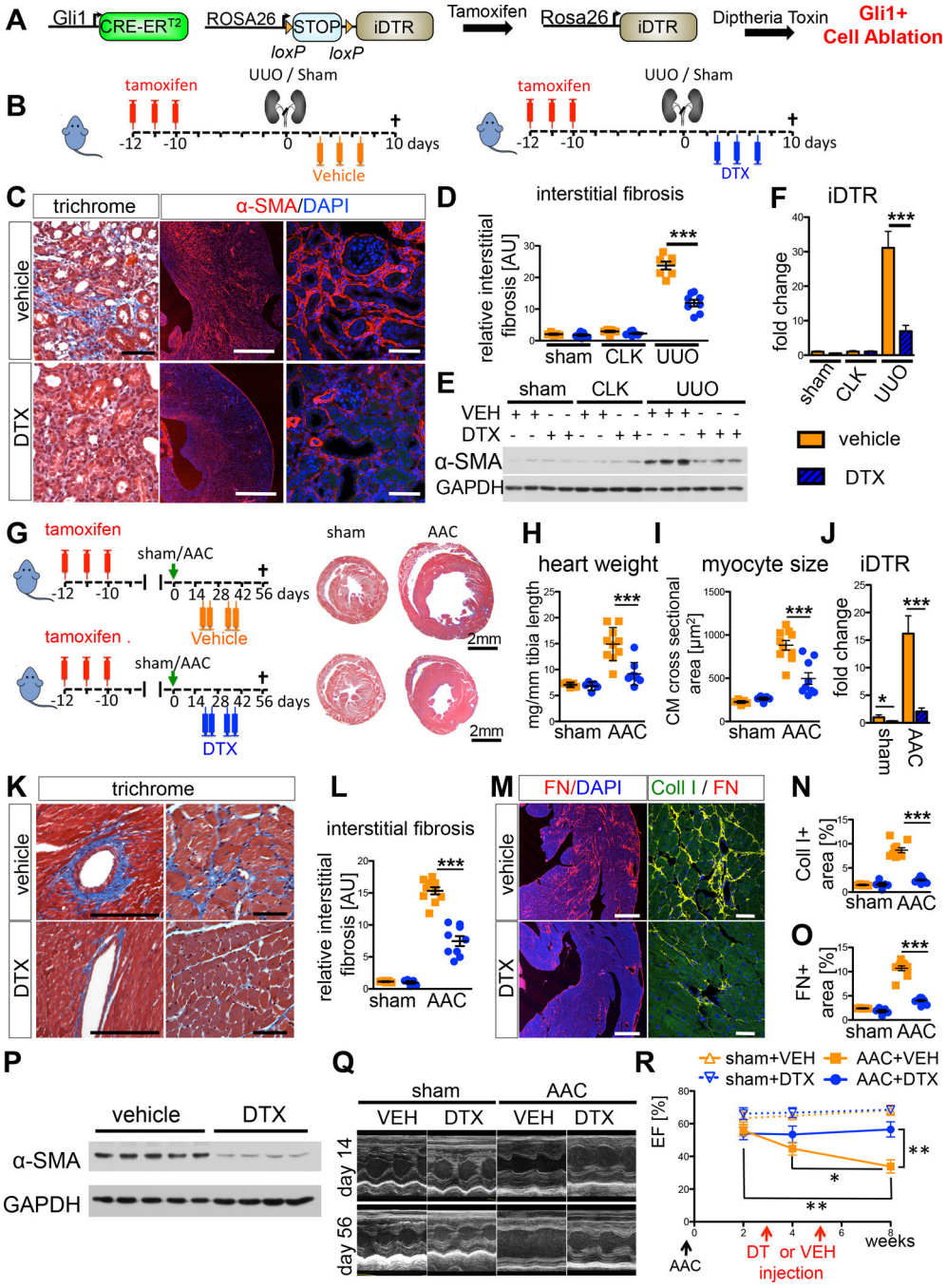

Figure 7. Ablation of Gli1$^+$ cells via the human diphtheria toxin receptor ameliorates kidney and heart fibrosis and rescues left ventricular function in heart failure

(A) Experimental scheme. Gli1CreER^{t2}; iDTR bigenic mice were administered tamoxifen, leading to heritable expression of the human DTR in Gli1$^+$ cells, allowing ablation of these cells via diphtheria toxin (DTX) injection.

(B) Gli1CreER^{t2}; iDTR mice were subjected to UUO or sham surgery, injected with vehicle (VEH=PBS) or DTX following surgery as indicated (n=5 sham + VEH, n=7 sham + DTX, n=7 UUO + VEH, n=8 UUO + DTX).

(C–E) Ablation of $Gli1^+$ cells by DTX reduced severity of kidney fibrosis following UUO as demonstrated by trichrome staining, immunostaining and western blotting for α-SMA and quantification of interstitial fibrosis. Scale bars: left two panels 500μm, others 50μm; ***p<0.001 by one way ANOVA with posthoc Tukey, mean ± SEM.

(F) iDTR mRNA increases in UUO kidneys reflecting the expansion of $Gli1^+$; $iDTR^+$-cells, whereas DTX injection significantly reduced iDTR expression in UUO kidneys indicating ablation of $Gli1^+$,$iDTR^+$ cells; ***p<0.001 by t-test, mean ± SEM.

(G) $Gli1CreER^{t2}$; iDTR mice underwent ascending aortic constriction (AAC) or sham surgery and were randomized to subsequently receive either diphtheria-toxin (DTX, n=9 AAC, n=5 sham) or vehicle (PBS, n=10 AAC, n=5 sham). Note decreased heart size in DTX-treated mice.

(H–I) Ablation of $Gli1^+$ cells ameliorated cardiac hypertrophy as indicated by reduced heart weight and cardiomyocyte (CM) cross-sectional area (*p<0.05 by t-test, mean±SEM).

(J) Confirmation of ablation by reduction in mRNA for DTR receptor (*p<0.05 by t-test, mean ± SEM).

(K–L) Reduced interstitial fibrosis by trichrome stain following DTX injection. Scale bars: 50μm, ***p<0.001 by t-test; mean ± SEM.

(M–O) Reduced fibronectin and collagen-1 expression and quantification following DTX injection. Scale bars: 500μm left panel, 50μm right panel; ***p<0.001 by t-test.

(P) Reduced α–SMA following DTX injection.

(Q–R) After AAC, vehicle injected mice developed progressive heart failure, as expected (representative echocardiographic M-mode pictures in Q) with significantly reduced left ventricular ejection fraction (EF) at 8 weeks. Ablation of Gli1+ cells by DTX treatment rescued this progressive heart failure. *p<0.05; **p<0.01 by t-test, mean ± SEM, see also figure S6.